VIP *The following Communications have been judged by at least two referees to be "very important papers" and will be published online at www.angewandte.org soon:*

*T. Lewis, M. Faubel, B. Winter, J. C. Hemminger**
CO_2 Capture in an Aqueous Solution of an Amine: Role of the Solution Interface

*Y. H. Kim, S. Banta**
Complete Oxidation of Methanol in an Enzymatic Biofuel Cell by a Self-Assembling Hydrogel Created from Three Modified Dehydrogenases

*I. Coin, M. H. Perrin, W. W. Vale, L. Wang**
Photo-Cross-Linkers Incorporated into G-Protein-Coupled Receptors in Mammalian Cells: A Ligand Comparison

*S. Kawamorita, H. Ohmiya, T. Iwai, M. Sawamura**
Palladium-Catalyzed Borylation of Sterically Demanding Aryl Halides with a Silica-Supported Compact Phosphane Ligand

*F. Freire, A. M. Almeida, J. D. Fisk, J. D. Steinkruger, S. H. Gellman**
Impact of Strand Length on the Stability of Parallel-β-Sheet Secondary Structure

*K. A. B. Austin, E. Herdtweck, T. Bach**
Intramolecular [2+2]-Photocycloaddition of Substituted Isoquinolones: Enantioselectivity and Kinetic Resolution Induced by a Chiral Template

*S.-H. Kim, D. A. Weitz**
One-Step Emulsification of Multiple Concentric Shells with Capillary Microfluidic Devices

*O. V. Zenkina, E. C. Keske, R. Wang, C. Crudden**
Double Single-Crystal-to-Single-Crystal Transformation and Small-Molecule Activation in Rhodium NHC Complexes

Author Profile

"The best stage in a scientist's career is ALWAYS. Each has different opportunities, rewards, and challenges.
My favorite place on earth is the waves in front of Waikiki beach on a day when there is a 3–7 ft (Hawaiian scale) swell …"
This and more about Uwe H. F. Bunz can be found on page 7728.

News

R. Horn

S. Schauermann

P. H. Seeberger

Obituaries

William Nunn Lipscomb, Jr. (1919–2011)

Books

Magic Bullets to Conquer Malaria — Irwin W. Sherman

Highlights

Asymmetric Catalysis

S.-X. Huang, K. Ding* **7734 – 7736**

Asymmetric Bromoamination of Chalcones with a Privileged *N*,*N*′-Dioxide/Scandium(III) Catalyst

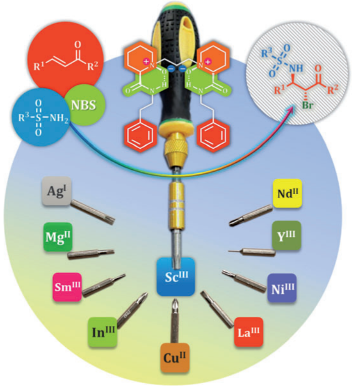

Choice of metal tips: A scandium(III) complex of a chiral *N*,*N*′-dioxide ligand demonstrated excellent regio-, diastereo-, and enantioselectivity, as well as exceptionally high activity in the first catalytic asymmetric bromoamination of chalcone derivatives (see picture). The products, α-bromo-β-amino ketones, have synthetic utility.

Total Synthesis

M. Szostak, D. J. Procter* **7737 – 7739**

Concise Syntheses of Strychnine and Englerin A: the Power of Reductive Cyclizations Triggered by Samarium Iodide

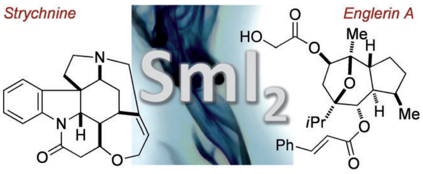

Electronica: Spectacular cyclization reactions mediated by the electron-transfer reagent samarium diiodide (Kagan's reagent) were instrumental in efficient syntheses of the classic alkaloid strychnine and the recently discovered guaiane sesquiterpene, englerin A (see picture).

Minireviews

Cyclobutanes

T. Seiser, T. Saget, D. N. Tran, N. Cramer* **7740 – 7752**

Cyclobutanes in Catalysis

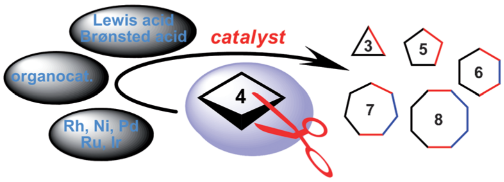

Fantastic four: The ring strain of cyclobutane is an excellent motor for the discovery of novel reactivity. This Minireview highlights recent developments in catalytic processes involving four-membered rings (see picture). In particular, transition-metal-promoted C–C bond-activation and β-carbon-elimination processes, which enable exciting downstream reactions, have made cyclobutane derivatives versatile substrates.

For the USA and Canada: ANGEWANDTE CHEMIE International Edition (ISSN 1433-7851) is published weekly by Wiley-VCH, PO Box 191161, 69451 Weinheim, Germany. Air freight and mailing in the USA by Publications Expediting Inc., 200 Meacham Ave., Elmont, NY 11003. Periodicals postage paid at Jamaica, NY 11431. US POSTMASTER: send address changes to *Angewandte Chemie*, Journal Customer Services, John Wiley & Sons Inc., 350 Main St., Malden, MA 02148-5020. Annual subscription price for institutions: US$ 11.738/10.206 (valid for print and electronic / print or electronic delivery); for individuals who are personal members of a national chemical society prices are available on request. Postage and handling charges included. All prices are subject to local VAT/sales tax.

Reviews

Substitute O for N: The renaissance and development of nitridosilicates and related compounds is presented (see picture). Beginning with functional ceramics, the review then presents the remarkable spectrum of structural features and versatile applications as functional materials, most notably upon doping with Eu^{2+} in phosphor-converted LEDs.

Ceramic Materials

M. Zeuner, S. Pagano, W. Schnick* ——— **7754 – 7775**

Nitridosilicates and Oxonitridosilicates: From Ceramic Materials to Structural and Functional Diversity

Communications

Triple-crossed: An extraordinary crossing reaction involving three popular utility organolithium reagents *n*BuLi, LiTMP (TMP = 2,2,6,6-tetramethylpiperidide), and LiC_5H_5 leads to the unexpected deprotonation of $C_5H_5^-$ anions to $C_5H_4^{2-}$ dianions, which was manifested through the trapping of the hexameric *n*BuLi cage by a $[\{Li(\mu\text{-}TMP)Li(\mu\text{-}C_5H_5)\}_4]$ molecular square ring (see picture).

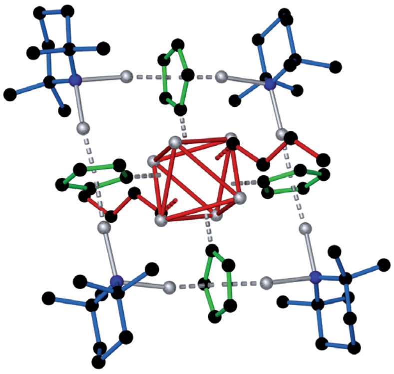

Organolithium Chemistry

A. A. Fyfe, A. R. Kennedy, J. Klett,* R. E. Mulvey ——— **7776 – 7780**

Crossing Organolithium Compounds with Organolithium Compounds: Molecular Squares and a Cage-Encapsulating Reaction

Biosynthesis as a model: Based on the branched structure of biosynthetic pathways, such as the shikimate pathway, the selective bioproduction of a set of diverse metabolites has been achieved by means of metabolic engineering (see scheme). A scale-up for preparative purposes was performed, resulting in high product titers and yields from renewable resources.

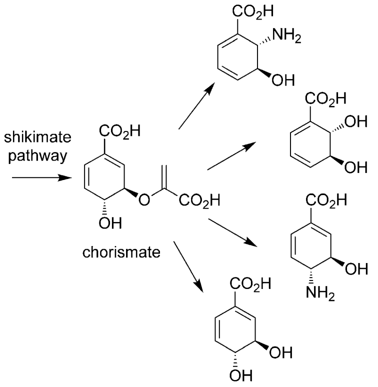

Synthetic Biology

J. Bongaerts, S. Esser, V. Lorbach, L. Al-Momani, M. A. Müller, D. Franke, C. Grondal, A. Kurutsch, R. Bujnicki, R. Takors, L. Raeven, M. Wubbolts, R. Bovenberg, M. Nieger, M. Schürmann, N. Trachtmann, S. Kozak, G. A. Sprenger,* M. Müller* ——— **7781 – 7786**

Diversity-Oriented Production of Metabolites Derived from Chorismate and Their Use in Organic Synthesis

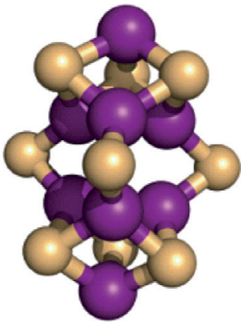

The fate of iron eight: The active site of Mo-nitrogenase is FeMoco. Previously, a FeMoco precursor was captured on NifEN, a scaffold protein for FeMoco biosynthesis. The FeMoco precursor is now isolated from the NifEN. The integrity of the precursor is shown by its full catalytic activity on incorporation into precursor-deficient NifEN. XAS/EXAFS analysis supports the eight-iron model of the precursor (see structure: Fe purple, S yellow).

Cofactors

VIP

A. W. Fay, M. A. Blank, C. C. Lee, Y. Hu,* K. O. Hodgson,* B. Hedman,* M. W. Ribbe* ——— **7787 – 7790**

Spectroscopic Characterization of the Isolated Iron–Molybdenum Cofactor (FeMoco) Precursor from the Protein NifEN

Synthetic Methods

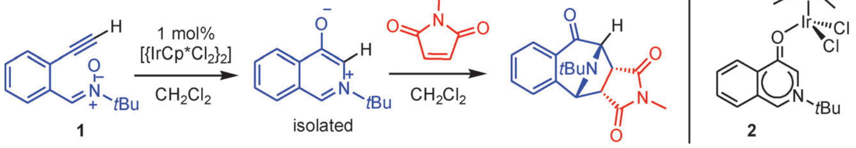

Cat. at rest: [$\{IrCp^*Cl_2\}_2$] readily catalyzes the redox cyclization of nitron alkynes (e.g., **1**) to give azomethine ylides that can then react with electrophiles and π bonds. The unusual O-bound azomethine complex **2** was isolated and identified as the resting state of the catalyst in the azomethine ylide formation. $Cp^* = C_5Me_5$.

Natural Product Biosynthesis

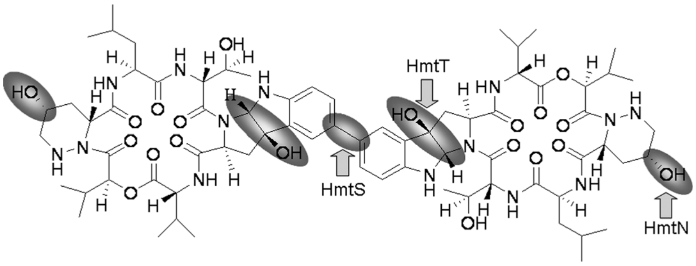

It's only natural: The biosynthetic pathway of himastatin from *Streptomyces himastatinicus* featuring unusual domain organizations is elucidated by genome scanning, generation of in-frame gene deletion mutants, and complementation experiments. Three cytochrome P450s that catalyze novel post-tailoring oxidative reactions (see picture) are characterized.

Nucleophilic Addition

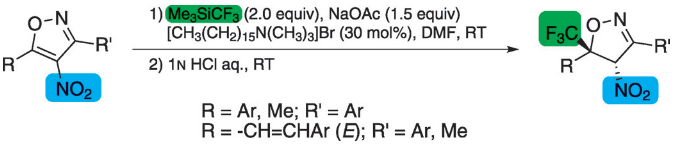

It all adds up: The activation of aromatic isoxazoles with a nitro group at the 4-position has enabled the first regio- and diastereoselective trifluoromethylation at the 5-position of isoxazoles by nucleophilic addition using Me_3SiCF_3 (see scheme; DMF = *N,N'*-dimethylformamide). The process was demonstrated with a broad range of 3,5-aromatic, heteroaromatic and aliphatic substrates.

Rotational Spectroscopy

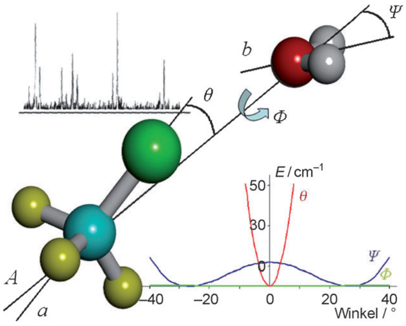

Molecular spinning tops: Five halogen-bonded isotopologues of the $CF_3Cl–H_2O$ complex have been assigned by Fourier-transform microwave spectroscopy. All complexes are symmetric-top systems with evenly spaced bonds. The free internal rotation, relative stability, and structure of these complexes were determined (see picture; Ψ, θ, and Φ: angles, *a* and *b*: axes of the monomer, and *A*: axis of the complex).

Nanocomposites

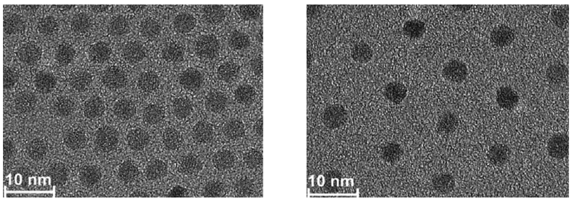

Mixing in: Attachment of a polymer-brush layer to the surface of nanoparticles makes the nanoparticles miscible with the polymer matrix. Adjusting the length of the attached polymer chains enables exact control of the distance between adjacent nanoparticles (see picture).

Sustainable Gold Catalysis

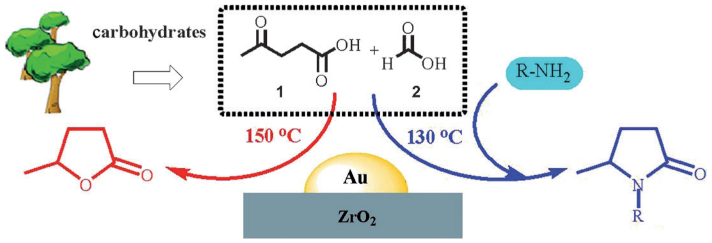

A golden opportunity: A highly robust catalyst system consisting of gold nanoparticles supported on acid-tolerant ZrO_2 promoted the conversion of biomass-derived levulinic acid (**1**) and formic acid (**2**) into γ-valerolactone without the use of an external H_2 supply (see scheme, red). The Au/ZrO_2 catalyst was also used for the direct one-pot synthesis of highly valuable pyrrolidone derivatives from **1**, **2**, and primary amines (see scheme, blue).

Gold Catalysis

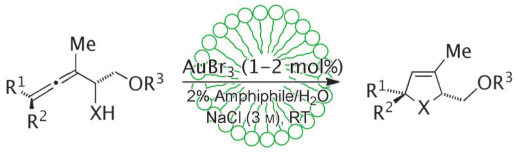

Micelles to the rescue: Two amphiphiles are shown to afford air-stable aqueous gold catalyst solutions with excellent reactivity and recyclability. Various α-functionalized allenes can be cycloisomerized smoothly and efficiently with this system at room temperature. Addition of NaCl to the reaction mixture affords larger micelles and induces faster reactions.

Ultrafast Photophysics

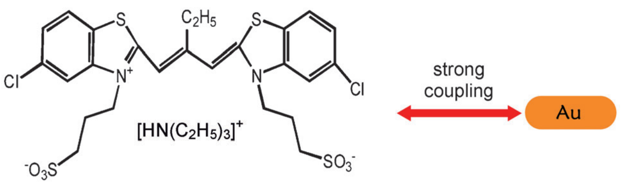

The photophysics of a molecule-coated gold nanorod structure was studied by ultrafast transient spectroscopy under resonant pumping. The results provide evidence for coherent coupling between the exciton and SP modes. The behavior is very similar to polaritons in an optical microcavity.

User-Friendly Catalysts

J. Heppekausen,
A. Fürstner* **7829 – 7832**

Rendering Schrock-type Molybdenum Alkylidene Complexes Air Stable: User-Friendly Precatalysts for Alkene Metathesis

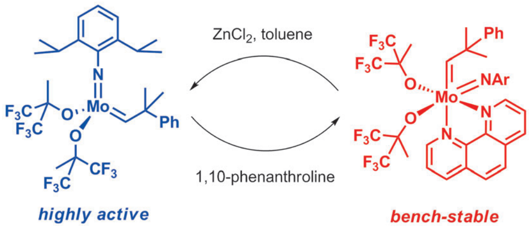

A matter of convenience: Schrock molybdenum alkylidenes are amongst the most powerful olefin metathesis catalysts known to date, but their sensitivity to air and moisture mandates their handling in a glove-box or by Schlenk techniques. This inconvenience is circumvented by using the corresponding phenanthroline- or bipyridine adducts, which are bench-stable and hence very user-friendly. The active species can be liberated from these precatalysts in uncompromised form on treatment with ZnCl$_2$ in toluene (see scheme).

Energy Transfer

D. Hablot, A. Harriman,*
R. Ziessel* **7833 – 7836**

Using a Photoacid Generator to Switch the Direction of Electronic Energy Transfer in a Molecular Triad

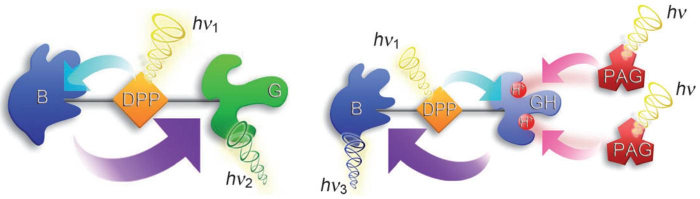

A switch in time: A sequence of highly efficient, intramolecular electronic energy transfer steps follows from selective illumination of the fluorescent center (DPP) present in a new class of molecular triads (see picture). The direction of energy flow depends on the protonation state of one of the termini (B and G), which can be modulated by direct or sensitized photolysis of a photoacid generator (PAG).

Asymmetric Synthesis

F. Zhong, X. Han, Y. Wang,
Y. Lu* **7837 – 7841**

Highly Enantioselective [3+2] Annulation of Morita–Baylis–Hillman Adducts Mediated by L-Threonine-Derived Phosphines: Synthesis of 3-Spirocyclopentene-2-oxindoles having Two Contiguous Quaternary Centers

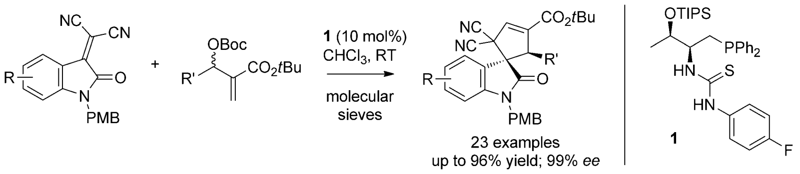

Spiral bound: The Morita–Baylis–Hillman adducts were employed as C$_3$ synthons in the asymmetric [3+2] annulation with malonitrile substrates using L-threonine-derived **1** as the catalyst (see scheme). The reaction is highly regioselective and stereoselective, and affords optically enriched 3-spirocyclopentene-2-oxindoles containing two contiguous quaternary centers. Boc = *tert*-butoxycarbonyl, PMB = *para*-methoxybenzyl, TIPS = triisopropylsilyl.

Organocatalysis

A. Gualandi, E. Emer, M. G. Capdevila,
P. G. Cozzi* **7842 – 7846**

Highly Enantioselective α Alkylation of Aldehydes with 1,3-Benzodithiolylium Tetrafluoroborate: A Formal Organocatalytic α Alkylation of Aldehydes by the Carbenium Ion

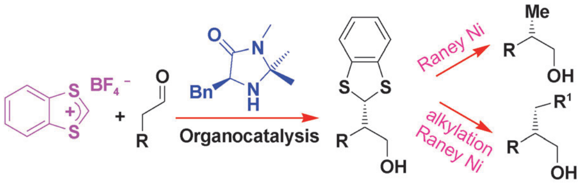

A formal formyl: The organocatalytic stereoselective addition of formyl equivalents to aldehydes (see scheme) tolerates a large variety of functional groups to afford products with high enantioselectivity (92–97 % *ee*) and good yields (up to 95 %). The benzodithiol group can be easily removed with Raney Ni or metalated with *n*BuLi, thus giving access to a methyl group or to a wide range of useful intermediates.

Stacking Interactions

J. W. G. Bloom,
S. E. Wheeler* 7847 – 7849

Taking the Aromaticity out of Aromatic Interactions

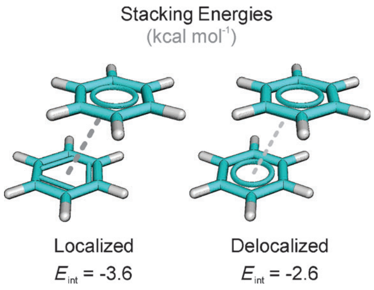

What's in a name? The phrase "aromatic interactions" is widely used to describe noncovalent interactions involving aromatic rings. However, computed stacking energies suggest that disruption of the aromatic π delocalization can enhance many of these interactions and also render them orientation-dependent. Because of these effects, the use of nonaromatic systems should be advantageous in supramolecular chemistry.

Nanoparticles

M. Jin, H. Zhang, Z. Xie,
Y. Xia* 7850 – 7854

Palladium Concave Nanocubes with High-Index Facets and Their Enhanced Catalytic Properties

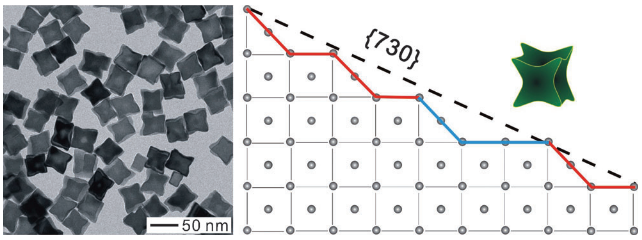

Curvy cubes: Palladium concave nanocubes enclosed by high-index {730} facets were obtained in high purity by controlling the overgrowth of Pd cubic seeds (see scheme). The concave nanocubes showed a much higher catalytic activity than the conventional Pd nanocubes enclosed by {100} facets for both electro-oxidation of formic acid and Suzuki coupling reaction.

Natural Product Synthesis

C. M. Schneider, K. Khownium, W. Li,
J. T. Spletstoser, T. Haack,
G. I. Georg* 7855 – 7857

Synthesis of Oximidine II by a Copper-Mediated Reductive Ene–Yne Macrocyclization

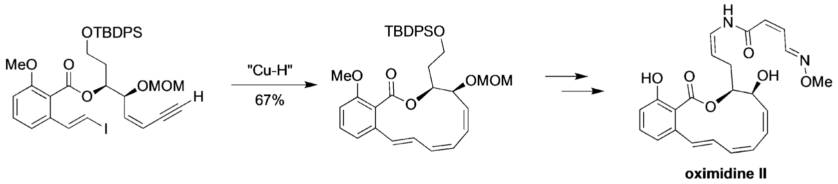

Holy macro! An intramolecular copper-mediated reductive Castro–Stephens reaction furnished a key macrocyclic triene intermediate for the total synthesis of oximidine II (see scheme). The total synthesis of the natural product was completed and the mechanism of this unprecedented key reaction was deduced.

Metallodrug Mechanosynthesis

V. André, A. Hardeman, I. Halasz,
R. S. Stein, G. J. Jackson, D. G. Reid,
M. J. Duer, C. Curfs, M. T. Duarte,
T. Friščić* 7858 – 7861

Mechanosynthesis of the Metallodrug Bismuth Subsalicylate from Bi_2O_3 and Structure of Bismuth Salicylate without Auxiliary Organic Ligands

Ground out: Mechanochemical methods gave the pharmaceutical ingredient bismuth subsalicylate, as well as bismuth disalicylate and trisalicylate directly from bismuth oxide. Structure determination by powder X-ray diffraction gave the first structure of a bismuth salicylate without auxiliary organic ligands (see picture: Bi yellow, O red, C gray, two salicylate ion coordination modes are shown in purple and green).

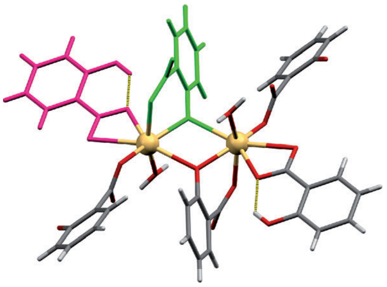

Natural Product Synthesis

S. Fujii, S. Y. Chang,
M. D. Burke* **7862 – 7864**

Total Synthesis of Synechoxanthin through Iterative Cross-Coupling

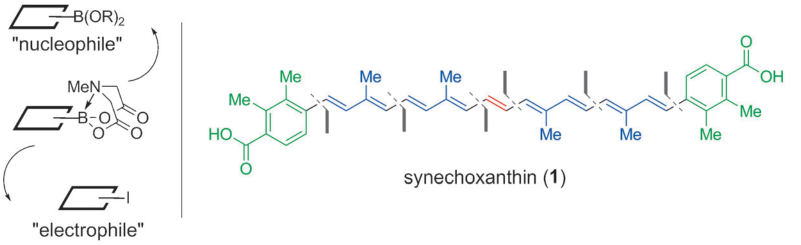

The choice is yours: The first total synthesis of the antioxidant carotenoid synechoxanthin was achieved through a novel iterative cross-coupling approach in which the polarity of the bifunctional building blocks is reversed to match the preferred polarity for C–C bond formation (see scheme). The convergent, stereocontrolled, and flexible nature of this synthesis enables systematic studies of the biological activities of this natural product.

Liquid Crystals

D. Miyajima, F. Araoka, H. Takezoe,*
J. Kim, K. Kato, M. Takata,
T. Aida* **7865 – 7869**

Electric-Field-Responsive Handle for Large-Area Orientation of Discotic Liquid-Crystalline Molecules in Millimeter-Thick Films

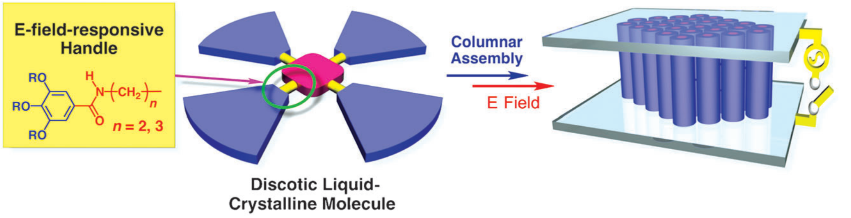

Current events: An electric-field-responsive handle (see picture) was developed that enables large-area and millimeter-thick unidirectional orientation of columnarly assembled π-conjugated liquid-crystalline molecules. The handles in the columns are hydrogen-bonded and align along the direction of an applied electric field.

Proton-Conducting Materials

M. Yoon, K. Suh, H. Kim, Y. Kim,
N. Selvapalam, K. Kim* **7870 – 7873**

High and Highly Anisotropic Proton Conductivity in Organic Molecular Porous Materials

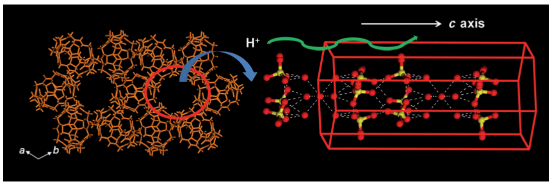

Cucurbituril-based organic molecular porous materials with 1D channels filled with water–acid arrays were synthesized. The isostructural materials showed different proton conductivity depending on the nature and number of acid molecules present in the channels. The highly anisotropic conduction behavior of the materials was studied by single-crystal conductivity measurements.

Reaction Mechanisms

J.-L. Zhou, Y. Liang, C. Deng, H. Zhou,
Z. Wang, X.-L. Sun, J.-C. Zheng, Z.-X. Yu,*
Y. Tang* **7874 – 7878**

Tunable Carbonyl Ylide Reactions: Selective Synthesis of Dihydrofurans and Dihydrobenzoxepines

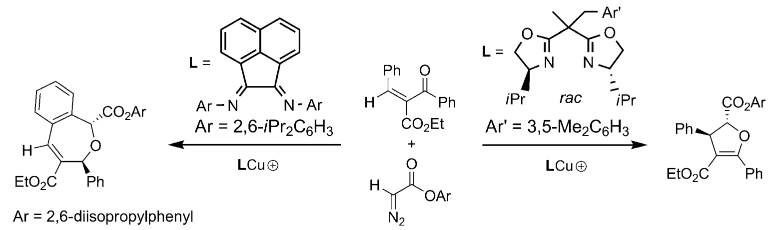

A select route: By selecting the appropriate ligand, dihydrofurans and dihydrobenzoxepines can be chemoselectively formed in moderate to good yields with good to excellent diastereocontrol from identical starting materials (see scheme).

Two-Dimensional Structures

T. Bauer, Z. Zheng, A. Renn, R. Enning, A. Stemmer, J. Sakamoto,* A. D. Schlüter* ______ **7879 – 7884**

Synthesis of Free-Standing, Monolayered Organometallic Sheets at the Air/Water Interface

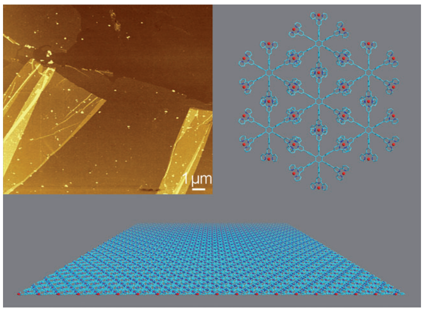

Sheets and rational synthesis are not like fire and water! Hexafunctional terpyridine monomers can be laterally connected by metal salts to result in a mechanically stable, sheetlike entity that can be transferred from the air/water interface to a solid substrate (see the folded, ca. 1.4 nm thin film) and spanned over micrometer-sized holes. This result is considered an important step on the way to 2D polymers.

Acetogenin Cytotoxicity

C.-C. Liaw,* W.-Y. Liao, C.-S. Chen, S.-C. Jao, Y.-C. Wu, C.-N. Shen,* S.-H. Wu* ______ **7885 – 7891**

The Calcium-Chelating Capability of Tetrahydrofuranic Moieties Modulates the Cytotoxicity of Annonaceous Acetogenins

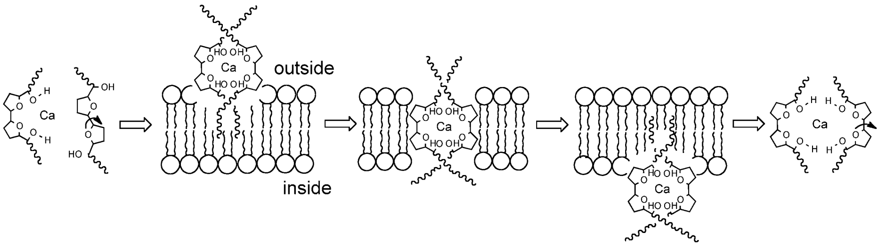

Forced entry: NMR spectroscopy and isothermal titration calorimetry show that calcium ions are chelated by the hydroxylated THF ring of acetogenins, which results in formation of complexes that aid the Ca^{2+} cations in penetrating cell membranes and in elevating the intracellular calcium level (see picture). This disruption of intracellular calcium homeostasis induces mitochondrial depolarization and mediates cell toxicity.

Star Polymer Catalysts

T. Terashima,* A. Nomura, M. Ito, M. Ouchi, M. Sawamoto* ______ **7892 – 7895**

Star-Polymer-Catalyzed Living Radical Polymerization: Microgel-Core Reaction Vessel by Tandem Catalyst Interchange

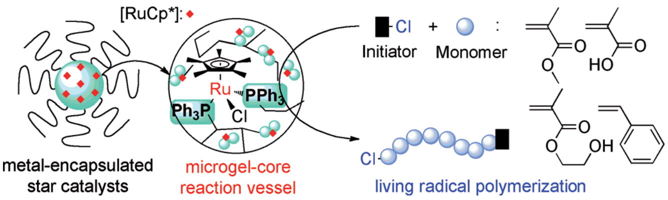

A star is born: Star polymer catalysts that carry a versatile microgel-core reaction vessel were obtained from catalyst interchange, coupled with ruthenium-catalyzed living radical polymerization, in situ hydrogenation, and removal and introduction of metals (see picture). Thanks to the catalyst encapsulation in the unique environment, the star catalysts show high activity, versatility, functionality tolerance, and recyclability in living radical polymerization.

Self-Assembly

I. Böhm, K. Isenbügel, H. Ritter,* R. Branscheid, U. Kolb ______ **7896 – 7899**

Cyclodextrin and Adamantane Host–Guest Interactions of Modified Hyperbranched Poly(ethylene imine) as Mimetics for Biological Membranes

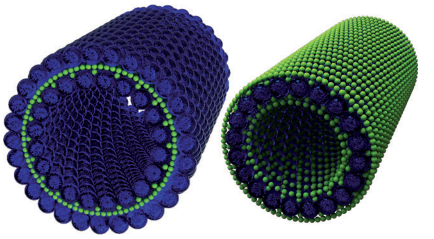

Take the tube: Mimetics for biological membranes formed by host–guest inclusion complexes were prepared from a cyclodextrin- and adamantyl-modified poly(ethylene imine) and a fluorescent dye (see picture). The tubular vesicles were quantitatively examined by fluorescence microscopy, cryo-TEM, and dynamic light scattering.

Contents

Heterogeneous Catalysis

A. Ghosh, S. Basak, B. H. Wunsch, R. Kumar, F. Stellacci* ______ **7900 – 7905**

Effect of Composition on the Catalytic Properties of Mixed-Ligand-Coated Gold Nanoparticles

Striped catalysts: The effect of composition and structure on the catalytic efficiency of gold nanoparticles protected by a monolayer composed of two types of ligands differing in length (see picture) is reported. By diluting catalytically active ligand molecules with simple catalytically inactive molecules the catalytic efficiency of the particles is enhanced.

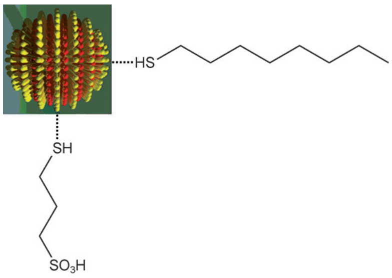

Phosphorus Ligands

C. H. Schuster, B. Li, J. P. Morken* ______ **7906 – 7909**

Modular Monodentate Oxaphospholane Ligands: Utility in Highly Efficient and Enantioselective 1,4-Diboration of 1,3-Dienes

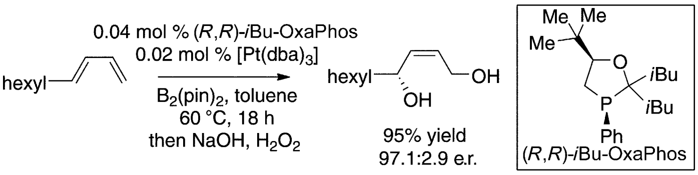

Tune it up! Tunable, chiral, monodentate oxaphospholane ligands (termed OxaPhos) are highly effective in the Pt-catalyzed title reaction, providing the 1,4-addition products in enantiomer ratios approaching 99:1 (see scheme). In the presence of enantiomerically pure *cis*-*i*Bu-OxaPhos, a catalyst loading of only 0.02 mol% $[Pt(dba)_3]$ was sufficient for effective reaction. pin = pinacolato, dba = dibenzylideneacetone.

Homogeneous Catalysis

Y. Yanagida, R. Yazaki, N. Kumagai,* M. Shibasaki* ______ **7910 – 7914**

Asymmetric Synthesis of Isothiazoles through Cu Catalysis: Direct Catalytic Asymmetric Conjugate Addition of Allyl Cyanide to α,β-Unsaturated Thioamides

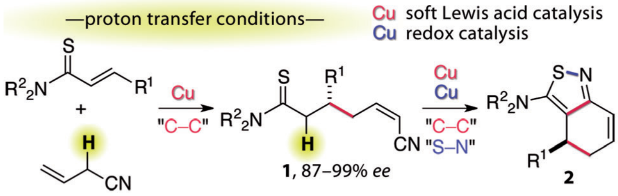

Twice the catalyst: The simultaneous activation of an allyl cyanide (pronucleophile) and an α,β-unsaturated thioamide (electrophile) was achieved using a Cu-based soft Lewis acid/hard Brønsted base cooperative catalyst, thus resulting in the formation of enethioamides **1** in a highly enantio- and *Z*-selective manner (see scheme). The sequential Cu-catalyzed intramolecular cyclization gave rise to enantioenriched fused isothiazoles **2**.

Immunosensors

B. S. Munge,* A. L. Coffey, J. M. Doucette, B. K. Somba, R. Malhotra, V. Patel, J. S. Gutkind, J. F. Rusling __ **7915 – 7918**

Nanostructured Immunosensor for Attomolar Detection of Cancer Biomarker Interleukin-8 Using Massively Labeled Superparamagnetic Particles

A sensitive issue: Superparamagnetic particle–antibody conjugates enable detection of interleukin-8 (IL-8) in serum at a level of 1 fg mL^{-1} (ca. 100 aM). Ultrahigh sensitivity is facilitated by a nanostructured sensor platform coupled with secondary antibody–magnetic bead–horseradish peroxidase conjugate (Ab_2–MB–HRP) with about 500 000 HRP labels (see picture).

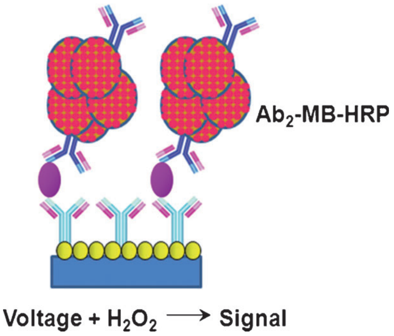

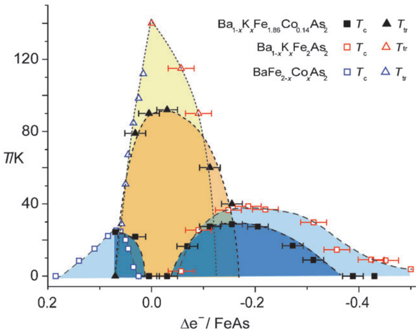

Superconductivity in doped $BaFe_2As_2$ is controlled by the charge of the $(FeAs)^{\delta-}$ layers. Adjustment from electron to hole doping in $Ba_{1-x}K_xFe_{1.86}Co_{0.14}As_2$ tailors the system from superconductivity to static magnetic order and back to superconductivity. When the charges compensate each other, the magnetic phase similar to $BaFe_2As_2$ is recovered. Structural parameters play minor roles in the superconductivity but are important for the highest possible critical temperatures.

Superconductivity

V. Zinth, T. Dellmann, H.-H. Klauss, D. Johrendt* **7919 – 7923**

Recovery of a Parentlike State in $Ba_{1-x}K_xFe_{1.86}Co_{0.14}As_2$

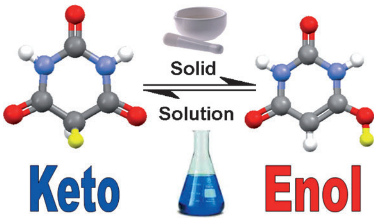

Stabilizing the unstable: In textbooks barbituric acid is always drawn in its keto tautomeric form, which is indeed preferred in solution and in most polymorphic phases. However, phase IV, obtained by grinding, consists of molecules in the enol form, as shown by neutron powder diffraction. This phase is found to be the most stable one at room temperature; the "unstable" enol tautomer is stabilized by a higher number of hydrogen bonds.

Keto–Enol Tautomerism

M. U. Schmidt,* J. Brüning, J. Glinnemann, M. W. Hützler, P. Mörschel, S. N. Ivashevskaya, J. van de Streek, D. Braga, L. Maini,* M. R. Chierotti,* R. Gobetto **7924 – 7926**

The Thermodynamically Stable Form of Solid Barbituric Acid: The Enol Tautomer

Hydrogen bonds involving phosphate groups as acceptors only occur in noncanonical structure elements of RNAs and are important for their stable folding. These hydrogen bonds can be directly assigned by H,P correlation experiments in solution NMR spectroscopy owing to the presence of sizeable $^{2h}J_{HP}$ scalar couplings across the hydrogen bond. These experiments will provide valuable information to speed up the determination of complex RNA structures.

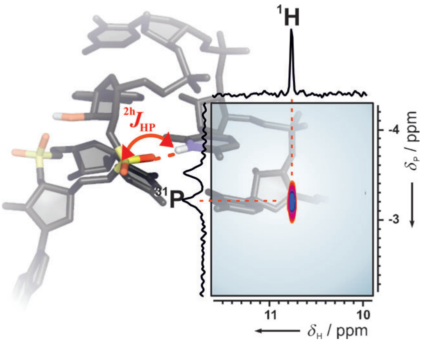

RNA Structure Elucidation

E. Duchardt-Ferner, J. Ferner, J. Wöhnert* **7927 – 7930**

Rapid Identification of Noncanonical RNA Structure Elements by Direct Detection of OH···O=P, NH···O=P, and NH_2···O=P Hydrogen Bonds in Solution NMR Spectroscopy

The pick of the pockets: The first inhibitors for IspD, an enzyme from the non-mevalonate pathway of isoprenoid biosynthesis, are described. High-throughput-screening revealed a hit with an IC_{50} value of 140 nM. Co-crystal structure analyses of the binding mode in the newly formed allosteric pocket (see structure, red ball: water O atom), lead to the synthesis of a set of 17 derivatives which were tested to optimize the herbicidal activity.

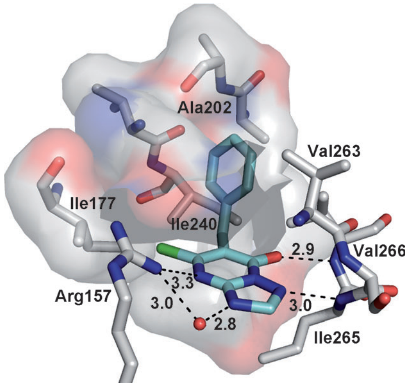

Herbicides

M. C. Witschel,* H. W. Höffken, M. Seet, L. Parra, T. Mietzner, F. Thater, R. Niggeweg, F. Röhl, B. Illarionov, F. Rohdich, J. Kaiser, M. Fischer,* A. Bacher,* F. Diederich* **7931 – 7935**

Inhibitors of the Herbicidal Target IspD: Allosteric Site Binding

Contents

Silicon Clusters

K. Abersfelder, A. J. P. White,
R. J. F. Berger, H. S. Rzepa,
D. Scheschkewitz* ________ **7936 – 7939**

A Stable Derivative of the Global Minimum on the Si_6H_6 Potential Energy Surface

Silicon shuffle minimizes energy: Isomerization of the dismutational isomer of hexasilabenzene (see structure; R = 2,4,6-$iPr_3C_6H_2$) produces the Si-bridged propellane, a stable representative of the global minimum on the Si_6H_6 energy surface, which, despite its mass, can be distilled without decomposition. Its halogenation proceeds in the bridgehead positions. Unprecedented ^{29}Si NMR data of the new Si_6R_6 isomer is explained with magnetically induced cluster currents.

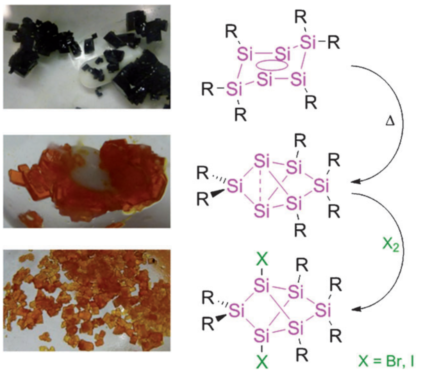

Chlorosulfolipids

C. Nilewski, N. R. Deprez, T. C. Fessard,
D. B. Li, R. W. Geisser,
E. M. Carreira* ____________ **7940 – 7943**

Synthesis of Undecachlorosulfolipid A: Re-evaluation of the Nominal Structure

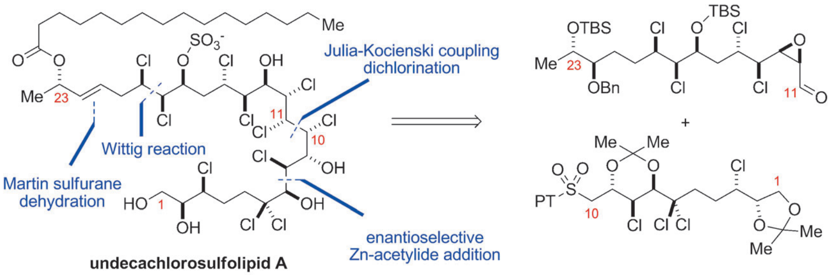

Halo-giant: The title compound at the left in the scheme was constructed by the synthesis and coupling of two stereochemically challenging fragments. A comparison of the NMR data of the synthetic material and the natural product indicates that the configuration had been misassigned in the latter. PT = 5-(1-phenyltetrazolyl).

Organocatalysis

G. Rulli, N. Duangdee, K. Baer,
W. Hummel, A. Berkessel,*
H. Gröger* ____________ **7944 – 7947**

Direction of Kinetically versus Thermodynamically Controlled Organocatalysis and Its Application in Chemoenzymatic Synthesis

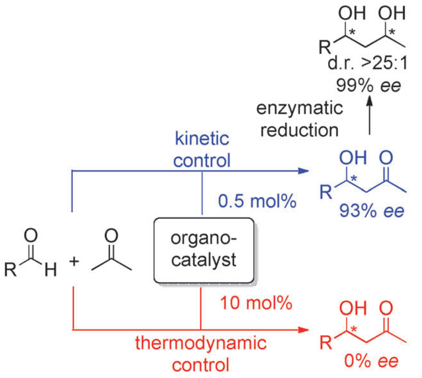

The catalyst loading in the narrow range between 0.5 and 10 mol% determines whether an enantioselective organocatalytic aldol reaction proceeds under kinetic or thermodynamic control; high conversions and *ee* values can be achieved with low catalyst loadings (see scheme). Since the reaction is carried out in water, it can be combined with a biocatalytic reduction for the one-pot synthesis of 1,3-diols with d.r. > 25:1 and 99% *ee*.

Phosphorus pulls its weight: Installation of a phosphoryl group as central bridge in the 4,4′-bipyridine scaffold introduces improved reduction responses that become even more pronounced in the corresponding phosphoryl-bridged methylviologen (see picture). Importantly, the scaffold maintains the typical viologen optical response upon reversible reduction, however, at much lower potentials.

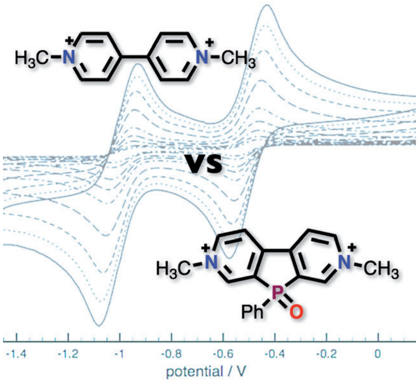

Supporting information is available on www.angewandte.org (see article for access details).

A video clip is available as Supporting Information on www.angewandte.org (see article for access details).

This article is available online free of charge (Open Access).

Service